Nuclear Materials and Energy 36 (2023) 101487

Contents lists available at ScienceDirect

Nuclear Materials and Energy

journal homepage: www.elsevier.com/locate/nme

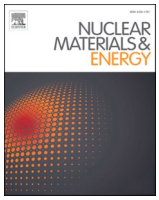

Electrophoretic deposition prepared yttria as interface of tungsten fiber reinforced tungsten composites

Y. Mao [a,*], A. Duggal [a,b], A. Dittes [b], T. Lampke [b], J.W. Coenen [a,c], Ch. Linsmeier [a]

[a] Forschungszentrum Jülich GmbH, Institut für Energie- und Klimaforschung - Plasmaphysik, Partner in the Trilateral Euregio Cluster, 52425 Jülich, Germany
[b] Materials and Surface Engineering Group, Institute of Materials Science and Engineering, Chemnitz University of Technology, D-09107 Chemnitz, Germany
[c] Department of Engineering Physics, University of Wisconsin Madison, WI, 53706, Madison, USA

ARTICLE INFO

Keywords:
Electrophoretic deposition
Yttrium oxide
Tungsten fiber reinforced tungsten composites
Microstructure

ABSTRACT

As the interface material for tungsten fiber reinforced tungsten composites (W_f/W), yttrium oxide thin films were prepared via an electrophoretic deposition (EPD) method in this study. The yttrium oxide dispersion is optimized based on its Zeta potential. The coating process was performed on the tungsten weaves (anode), and stainless steel was used as the counter electrode (cathode). The coating structure obtained from the EPD process was homogeneously distributed on all the fibers of the weave, but possess a porous structure. In addition, to optimize the coating process, the voltage influence on the coating process is demonstrated. Using the EPD prepared yttria interface, W_f/W is produced based on a chemical vapor deposition process. Initial mechanical test shows a promising property with extrinsic toughening mechanisms and high damage resilience.

Introduction

For future fusion reactor, the extreme operational condition pose a great challenge to the plasma facing materials [1]. Especially, the plasma facing materials for divertor will have to suffer cycled heat load (>10 MW/m^2 steady state for ITER, up to 1 GW/m^2 for transient heat load) under the condition of plasma erosion and neutron irradiation. Tungsten (W) is currently the most promising candidate for such application, since it is resilient against erosion, has the highest melting point of any metal and shows rather benign behavior under neutron irradiation [2,3]. Nevertheless, W is an intrinsic brittle material which could have the problem of cracking under the high cycled heat load [4]. Tungsten fiber reinforced tungsten composites (W_f/W) have been intensively developed to overcome the cracking issue of W. It has been reported that W_f/W can improve the damage tolerance of W relying on extrinsic toughening mechanisms [5–7]. Here, a dedicated weak interface between fiber and matrix plays a crucial role in realizing the designed energy dissipation during crack propagation [8,9]. Yttrium oxide is the currently most common interface material for W_f/W, due to its thermal and chemical stability, especially its low activation behavior [10–12], which is particularly important for nuclear application. In recent studies, yttrium oxide, as the interface of W_f/W, is mainly prepared by physical vapor deposition (PVD) [11,13] methods, which show promising coating quality and feasibility as the interface material for W_f/W. However, the production rate of the processes is relatively low, with high time and material consumption, which makes the preparation of the interface coating to be the bottleneck of W_f/W production [8].

Electrophoretic deposition (EPD) is a colloidal method in ceramic production and has advantages of brief formation time, needs simple apparatus, a little constraint of the substrate shape, no requirement for binder burnout as the green coating contains little or no organic substances [14]. The EPD method is very flexible compared to other advanced shaping methods since it can be easily changed for a specific application. For example, deposition can be made on flat, cylindrical, or any other shaped substrate with only minor changes in the design and positioning of the electrodes [15]. Despite being a wet process, in particular, EPD provides easy control of a deposited film's thickness and morphology through simple adjustment of the deposition time and the potential applied [16]. In EPD, dispersed or suspended charged powder particles in a liquid medium, are attracted and deposited upon application of a DC electric field on a conductive substrate of opposite charge. EPD is advantageous due to the reduced environmental impact, greater flexibility as well as lower operating costs, which promote the implementation of such procedures in larger-scale processes [17].

The ability of charged particles (such as colloidal particles) to move through a liquid medium in response to an electric field is known as

* Corresponding author.
E-mail address: y.mao@fz-juelich.de (Y. Mao).

https://doi.org/10.1016/j.nme.2023.101487
Received 16 June 2023; Received in revised form 5 August 2023; Accepted 14 August 2023
Available online 15 August 2023

Table 1
EPD parameters for yttrium oxide coating.

Exp.	Slurry Conc. (w %)	pH	Applied Voltage (V)	Time (min)	Drying Temp. (°C)	Drying Time (hours)
1	0.1%	10	10	15	100	24
2	0.1%	10	15	15	100	24
3	0.1%	10	20	15	100	24
4	0.1%	10	25	15	100	24
5	0.1%	10	30	15	100	24

electrophoretic mobility (μ_e) [18]. According to the theory of double layer, all surface charges in fluids are present by another layer of diffused ions with the same absolute charge but the opposite sign to the surface charges. In the diffuse layer, the electric field also exerts a force on the ions, which has an opposite direction to that basically acting on the surface charge. This latter force is then applied to the ions in the diffuse layer at some distance from the surface of the particle, not actually to the particle itself, but a part of it is transferred through viscous stress all the way to the surface of the particle. This part of the force is also referred to as electrophoretic retardation. So, when an electrical field is applied, the charged particle which is to be studied travels slowly through the diffuse layer. When a charged particle in a liquid is accelerated by a uniform electrical field until it reaches a steady drift velocity [19].

The Zeta potential of the suspended particles in a dispersion medium is a key factor in the EPD. Firstly, it plays a crucial role in stabilizing the dispersions by increasing the electrostatic repulsion between the charged particles in a dispersion medium, and secondly, the zeta potential helps in the determination of the migration direction and electrophoretic mobility [20]. In order to obtain the stabilized dispersions for EPD, a high Zeta potential (negative or positive) is required as it confers that the dispersion will resist the flocculation [16].

In this work, an electrophoretic deposition method was developed for yttrium oxide coatings on W fibers (weaves). The coating process was performed using an EPD cell with the tungsten weaves as anode and stainless-steel cathode in the yttrium oxide colloidal dispersion. The zeta potential of the dispersion and the deposition voltage were optimized. Afterwards, the EPD coated W weave was used to produce the W_f/W composites. Based on the preliminary mechanical test (one 3-point bending test), the W_f/W using EPD coated gives promising energy dissipation effects.

Methods and experiments

Dispersion preparation and Zeta potential measurement

To proceed with Electrophoretic deposition, the first step is to obtain stable dispersion of the nanoparticles. Yttrium Oxide nano dispersion (American Elements, APS < 100 nm, concentration 20 wt%) in distilled water is used in this study. As Zeta potential can be varied by adjusting the pH of the dispersion [21], Nitric Acid (65 %, Sigma Aldrich) and Sodium Hydroxide (Fisher Scientific) was used to adjust the pH of the dispersion. The obtained dispersion then was subjected to an ultrasonic bath for 30 min to achieve consistent dispersion in the dispersion.

The Zeta potential of the particles can be determined by measuring the movement speed of the particles under certain electric field, using the laser doppler electrophoresis [22]. In this study, to measure the Zeta potential of the nano-dispersions of Yttria, Zetasizer Nano ZS from Malvern Panalyticals was used with the Gold coated electrodes Zeta potential cell at Institute of Chemistry, TU Chemnitz Germany. Series of yttrium oxide dispersions with different pH value are measured.

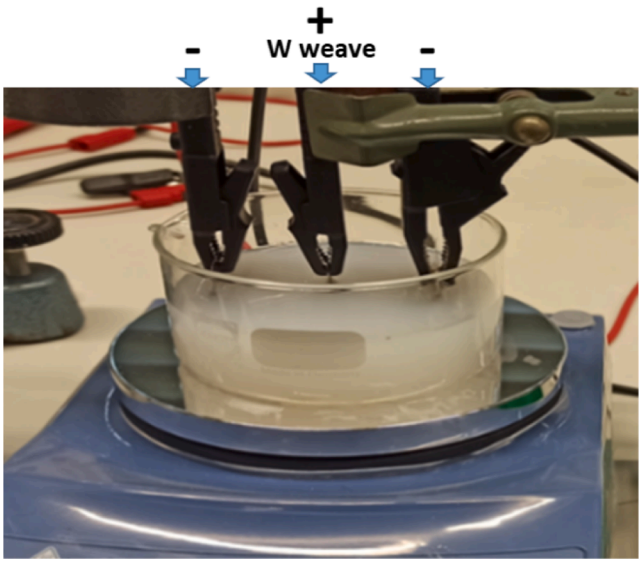

Fig. 1. The experimental setup showing the epd cell.

EPD process

After optimizing the yttrium oxide dispersion based on the adjustment of pH value and Zeta potential, the EPD process was performed. Two stainless steel electrodes were used as the counter electrodes and the deposition was done on tungsten weave substrates. Delta Elektronika SM300-5 as a DC power source (0–300 V) was used in the EPD experiments. The experiments were conducted in a voltage range of 10 V-30 V for 15 min, followed by a drying process. The prepared sample list is shown in Table 1. Fig. 1 shows (a) the setup, (b) the EPD cell for the experiments, and (c) an illustration of the EPD process, performed in this work. To investigate the high temperature stability of the EPD coated yttrium oxide layer, one of the weaves was annealed at 1000 °C for 1 h.

The surface morphology and cross-sectional analysis of the Y_2O_3 deposit on the Tungsten substrates were performed using Scanning electron microscopy (SEM, Carl Zeiss LEO 982), and Focused ion beam (FIB, Carl Zeiss Crossbeam 540 SEM), respectively. The chemical analysis of the deposited films was performed using energy-dispersive x-ray spectroscopy (EDX).

Production of W_f/W

To test the feasibility of the EPD prepared yttrium oxide coating as the interface between fiber and matrix, a single layer W_f/W composite was produced using a chemical vapor deposition (CVD) process using WF_6 as precursor in Forschungszentrum Jülich GmbH, Germany. The CVD process is reported in detail in [23]. Afterwards, the fracture behavior of the single layer W_f/W was tested using a 3-point bending test. The sample for the 3-point bending test is cut by wire cutting with a dimension of 20 × 3 × 2 mm (L × W × H). The fiber orientation is parallel to the sample length. After the 3-point bending test, the fracture section is observed by SEM.

Results and discussion

Zeta potential measurements

Zeta potential is one of the key parameters in the Electrophoretic deposition (EPD) [16]. The Zeta potential measurements were done by preparing the dispersions with different pH values, ranging from pH −1 to 14. The measured electrophoretic mobility, zeta potential and the stability of the Y_2O_3 dispersion are shown in Fig. 2. For the electrophoretic mobility, the value is negative through the whole pH range,

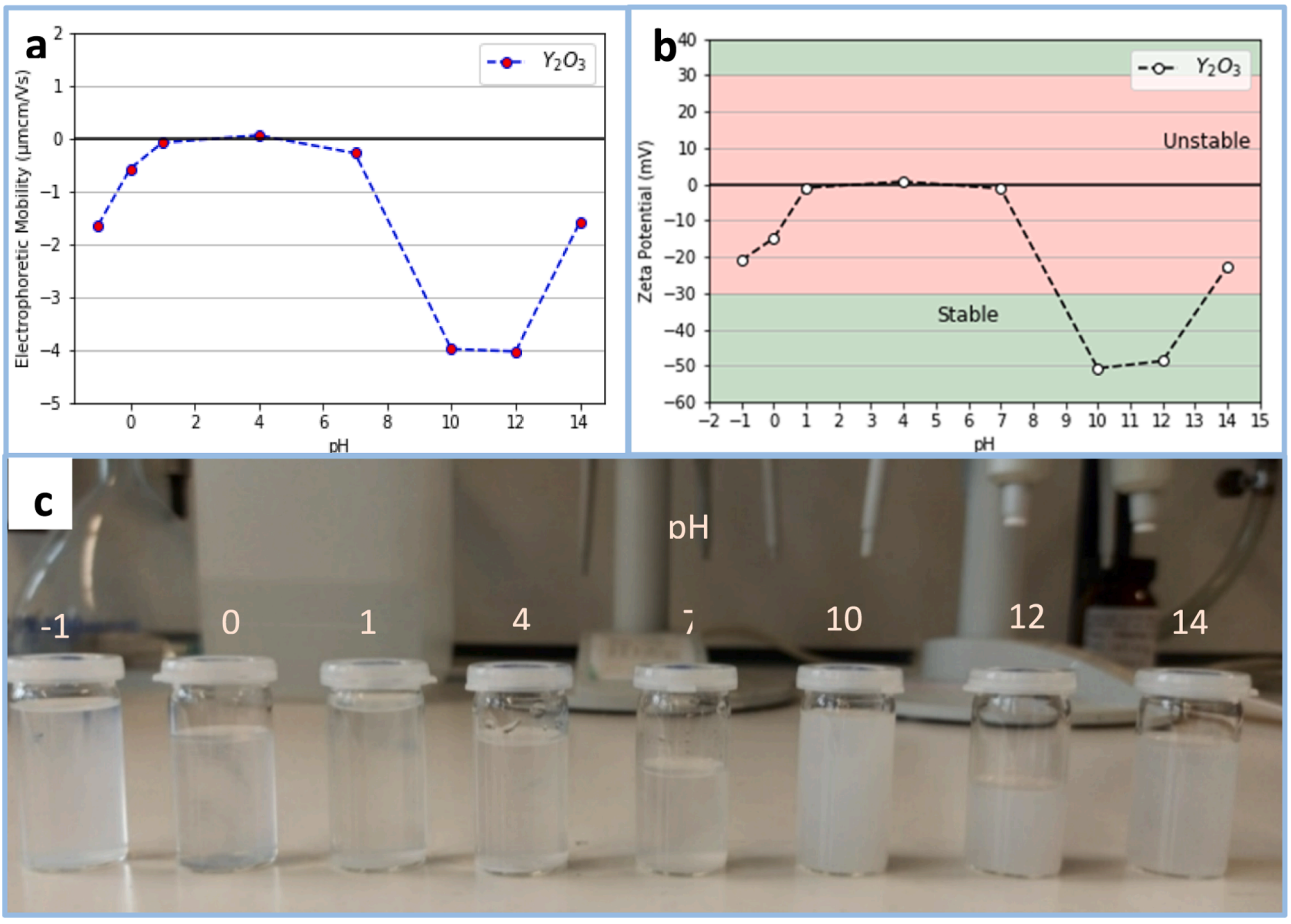

Fig. 2. Dispersion stabilization and the Zeta potential measurements of the 0.1 w% Y_2O_3 dispersion. (a) Electrophoretic mobility, (b) Zeta potential, (c) stabilization of the Y_2O_3 nanoparticles in the prepared dispersion with varied pH values.

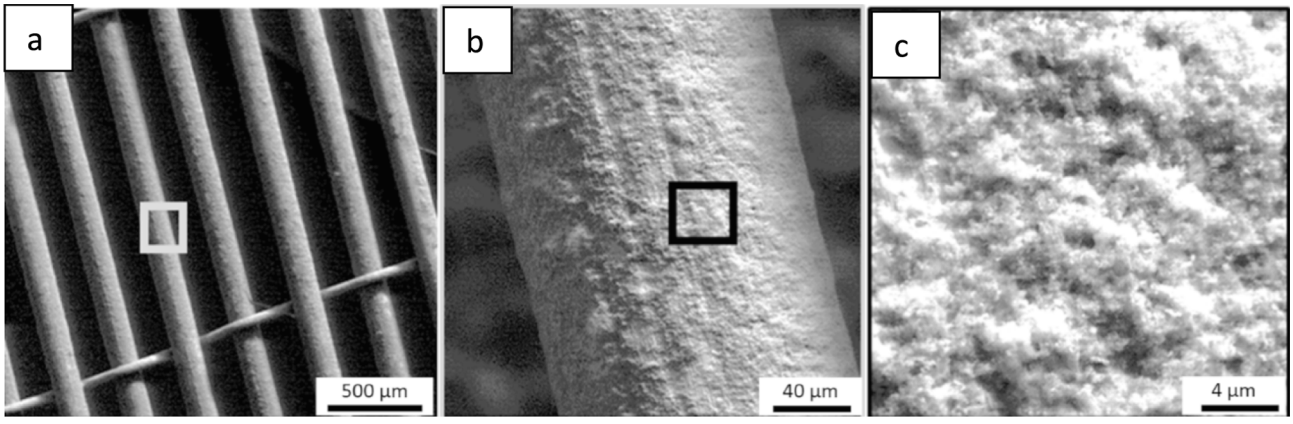

Fig. 3. Y_2O_3 EPD coating microstructure (surface) on the tungsten weaves deposited at 15 V for 15 min.

meaning that during the EPD process, the particles will move to the anode side. The absolute value reach the maximum at pH 10, giving that mobility/response of the particles in the electric field is high, which is beneficial to the EPD process. The colored zones in Fig. 2 (b) indicates the state of stabilization of the dispersions, red and green zones signify the unstable and stable degree of dispersions at different pH values for the measured Zeta potential. In Fig. 2 (c), obvious differences can be observed between the almost clear solutions (pH 0–7) and the very milky/cloudy solutions (pH 10–14). The particles have sedimented to the bottom of the beakers for the solutions pH 1–7, whereas the particles are still in the dispersion for the beakers at pH 10–14.

From the above-presented results of the Zeta potential measurement of the Y_2O_3 dispersions, it was observed that the dispersions are stabilized at two pH values, 10 and 12 with Zeta potential −51 mV and −48 mV, respectively. In the following studies, the dispersions are all with a pH value of 10. Given that the Zeta potential is in a negative range, the deposition of Y_2O_3 films were conducted on the anode.

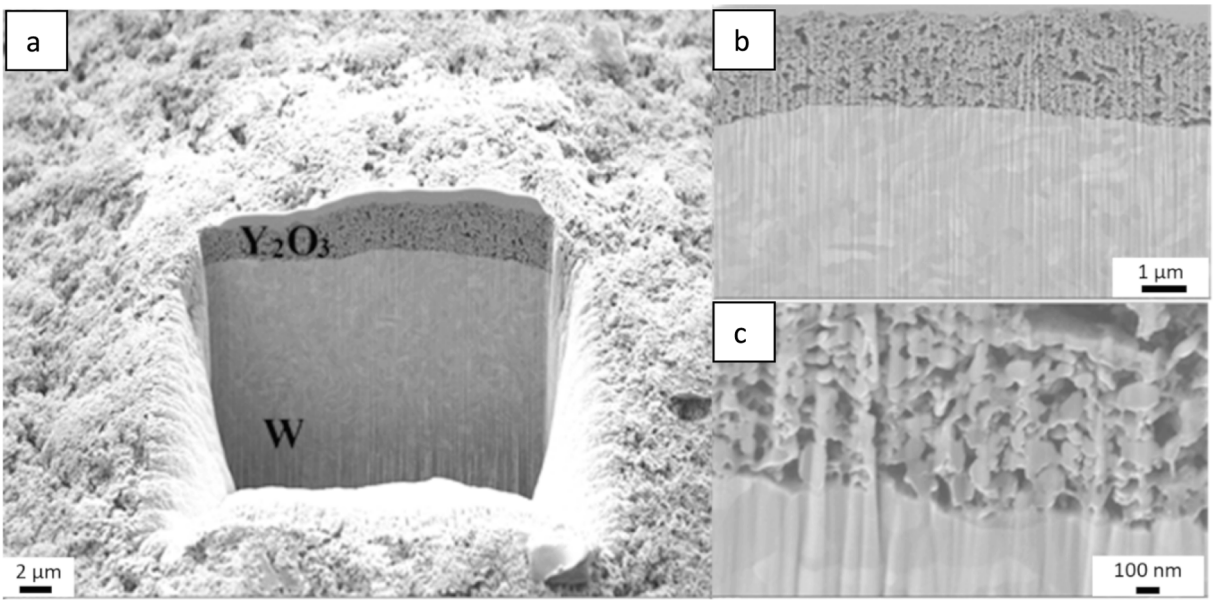

Fig. 4. SEM image of the FIB prepared coating cross section for the Y_2O_3 coated tungsten fiber, deposited at 15 V DC for 15 min.

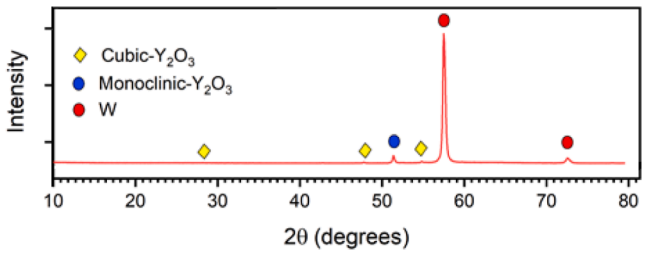

Fig. 5. X-Ray diffraction pattern on the Y_2O_3 coated tungsten weave by EPD process.

EPD coating on w-weaves

After coating process, the surface morphology of the coated weaves was analyzed by SEM. Fig. 3 gives the typical weave surface after EPD process (15 V, 15 min). The tungsten fibers in the weave have been coated entirely covering evenly the surface. The coating gives a porous morphology.

To further analyze the structural of the Y_2O_3 coatings on the tungsten weaves, a coating cross section was prepared by Focused Ion Beam (FIB). Fig. 4 shows a SEM image of a FIB prepared cross-section on a tungsten fiber coated with Y_2O_3 at 15 V DC for 15 min.

The Y_2O_3 coating on the tungsten fiber has a porous structure. At the interface of each particle and the W substrate, there seems to be a tight connection. The thickness of the coating deposited at 15 V DC for 15 min was about 2.5 μm. For this sample, apart from the surface morphological characterization, XRD analysis was performed on the specimens to identify the crystal structure of the deposited material. Fig. 5 presents

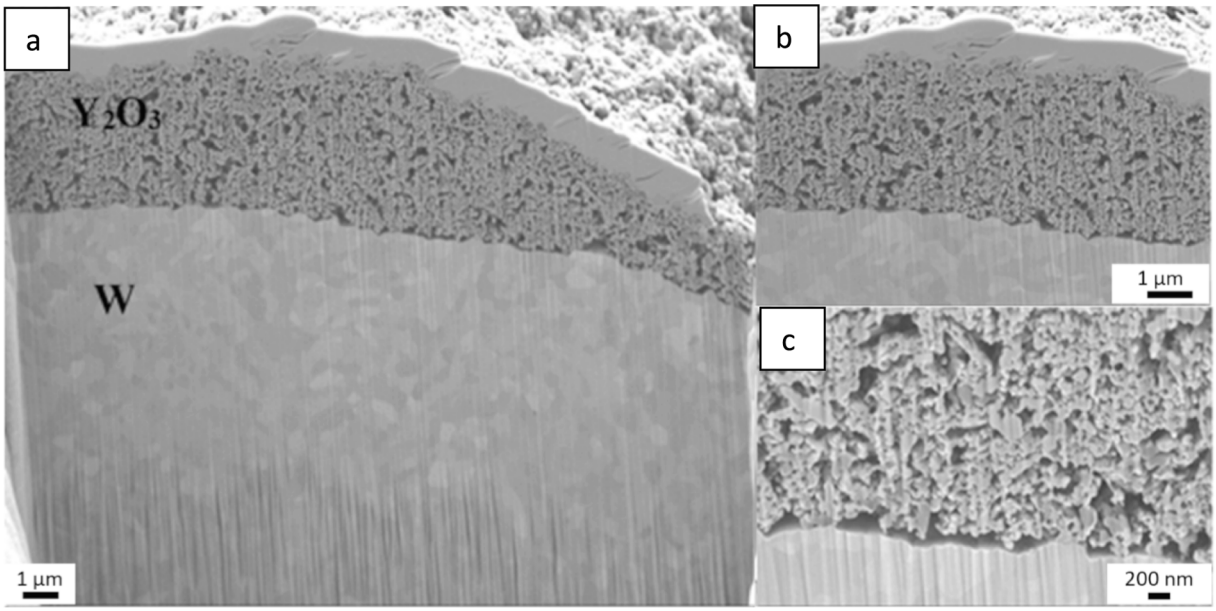

Fig. 6. Structural analysis of the Y_2O_3 coated tungsten fiber, annealed at 1000 °C.

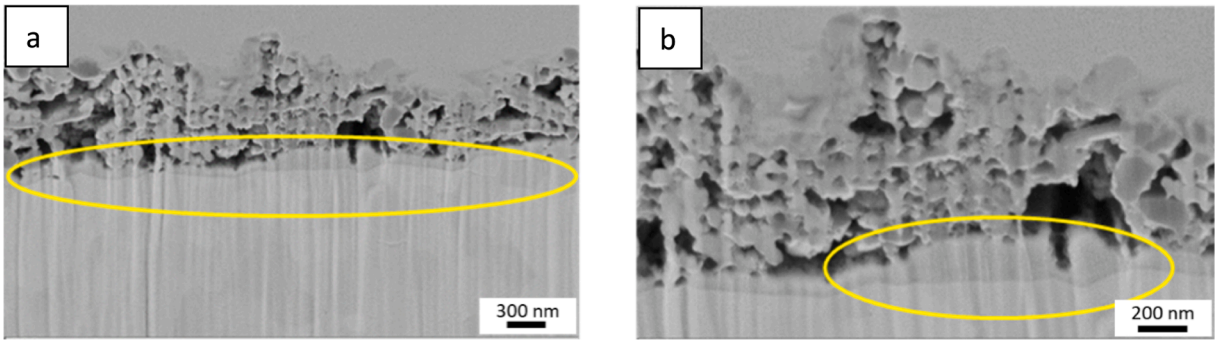

Fig. 7. SEM analysis of an additional layer at the interface of Y_2O_3 and Tungsten coated at 30 V.

the X-Ray Diffraction pattern with the Y_2O_3 and W peaks. During the XRD analysis, clear peaks of Yttrium Oxide (c-Y_2O_3) at $2\theta = 28.89$ and 48.08, and monoclinic phase (m-Y_2O_3) at $2\theta = 51.2$ were detected on the tungsten substrate.

After the EPD coating process, an annealing procedure was performed on the same specimen to stabilize the yttrium oxide structure. The annealing was carried out in a vacuum atmosphere at 1000 °C for 1 h. After the annealing process, the SEM analysis of FIB prepared cross-section of the abovementioned specimen is presented in Fig. 6. No signs of shrinkage, densification, cracking in the porous coating were found. A very similar microstructure of the deposited coating was observed after annealing, as that of the specimen without annealing. It is assumed that the high porosity allows for a compensation of thermally induced stresses during the annealing process, avoiding the coating delamination. The porous structure of the coating could be due to several possible reasons. Firstly, it could be that the nanoparticles in the dispersion are not separated and indeed are agglomerated; secondly, the porosity can also be explained from the successive deposition of individual particles during the EPD process; thirdly, the high porosity is linked to the not irregular shape of the particles. On the other hand the oxygen evolution from the water electrolysis on the anode could also be the reason the porous structure of the coating [24]. Nevertheless, the first requirement to achieve a homogeneous yttria coating on the tungsten fibers was met. With the repetition of the process at the same parameters the coating thickness of ~ 1——2.2 μm was achieved by EPD of the tungsten weave at 15 V DC. The reproducibility of the process has been proven by repeating the procedure.

For the films that coated at various voltage, no significant difference can be observed in terms of film structure. The coating thickness slightly increased with the increase in the applied electric field if the voltage is below 25 V. The coating deposited at 30 V showed a significant decrease in the thickness as compared to the specimens deposited at lower applied fields. An intermediate layer could be seen in the magnified SEM image of the tungsten specimen coated at 30 V, between the Y_2O_3 layer and the Tungsten surface (Fig. 7). This layer between the substrate surface and yttria coating could be an oxidization layer of the tungsten. This oxidation layer could be due to the electrolysis of water also the heat generation at the electrodes. For the process with a voltage higher than 25 V, a slow gas evolution on the anode side could be observed In this case, the 100–200 nm thick tungsten oxide layer is the typical barrier layer of the anodic oxidation–derived layer. This in turn might explain why the yttria deposit is significantly thinner than for 15 V deposition, as a part of the 30 V is used for the anodic oxidation reaction of tungsten and the rest of the voltage for the EPC process.

W_f/W production and mechanical testing

To test the feasibility of the EPD prepared yttrium oxide coating as the interface material for W_f/W, one W weave was coated by EPD process with 15 V for 15 min. Afterwards, a single layer W_f/W composite was produced using a CVD process. The microstructure of the prepared W_f/W and the interface are shown in Figure 8 and Fig. 9.

It can be seen that, for all the fibers in Figure 8, the interface are still visible after W coating by CVD process. Thermodynamically, Y_2O_3 can be reacted with WF_6 during the deposition process, and this can dissolve some interlayer materials [25], especially we have a porous coating here. We can see from Figure 8 and 9 that, there are some transition region at the outer shell of the coating. However, a dedicated Y_2O_3 interface still remain although the reaction time is quite long. It could be attributed the fact that, once certain amount W coating has been deposited, the Y_2O_3 will be covered with pure W and the reaction between Y_2O_3 and WF_6 can be retarded, leading to a self-limited effect. An EDS analysis on the interface region is shown in Fig. 10. It can be seen that, at the transition area on the outer shell of the interface, there is a clear W signal. But the yttrium signal can still be detected in this region. That means the infiltration of W into the porous coating. But as discussed above, a certain amount of Y_2O_3 dissolve is totally possible here. Nevertheless, the fibers and the matrix are effectively separated by the yttrium oxide coating.

The fracture behavior of the single layer W_f/W was tested using a 3-point bending test. The force–displacement curve is shown in Fig. 11. After the mechanical testing, the fracture section was observed by SEM, as shown in Fig. 12 (The tension side is the bottom in the figure).

The fracture behavior represents a typical pseudo ductility. After matrix failure, the W fibers take over the load, together with the interaction with the matrix, a catastrophic failure is avoid. Relying on various

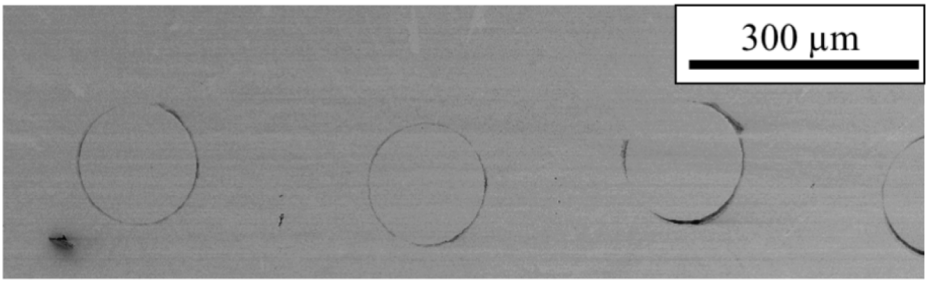

Fig. 8. Typical microstructure overview of the single layer w_f/W prepared by CVD process with EPD coated Yttrium oxide interface.

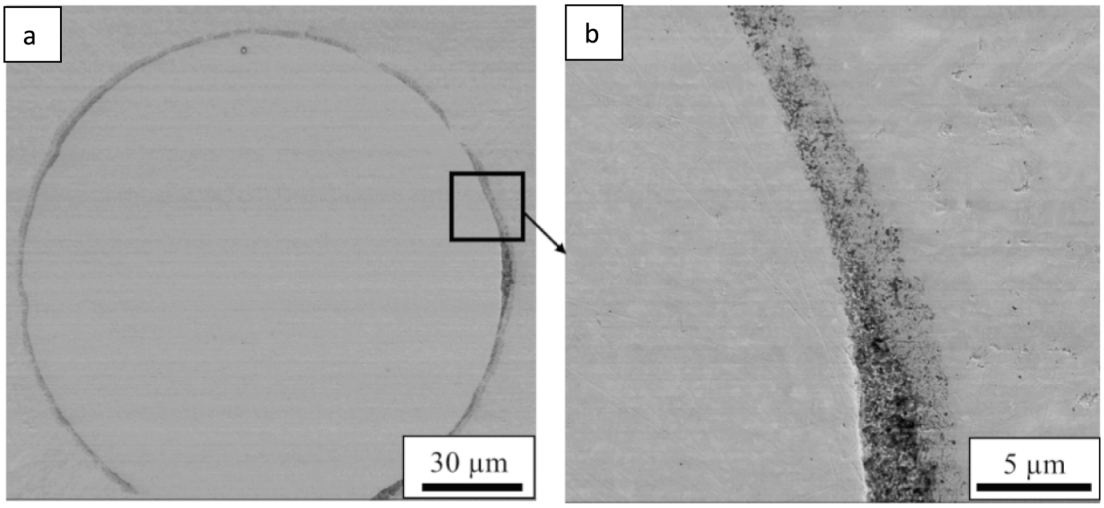

Fig. 9. The interface microstructure of the single layer w_f/W prepared by CVD process with EPD coated Yttrium oxide interface.

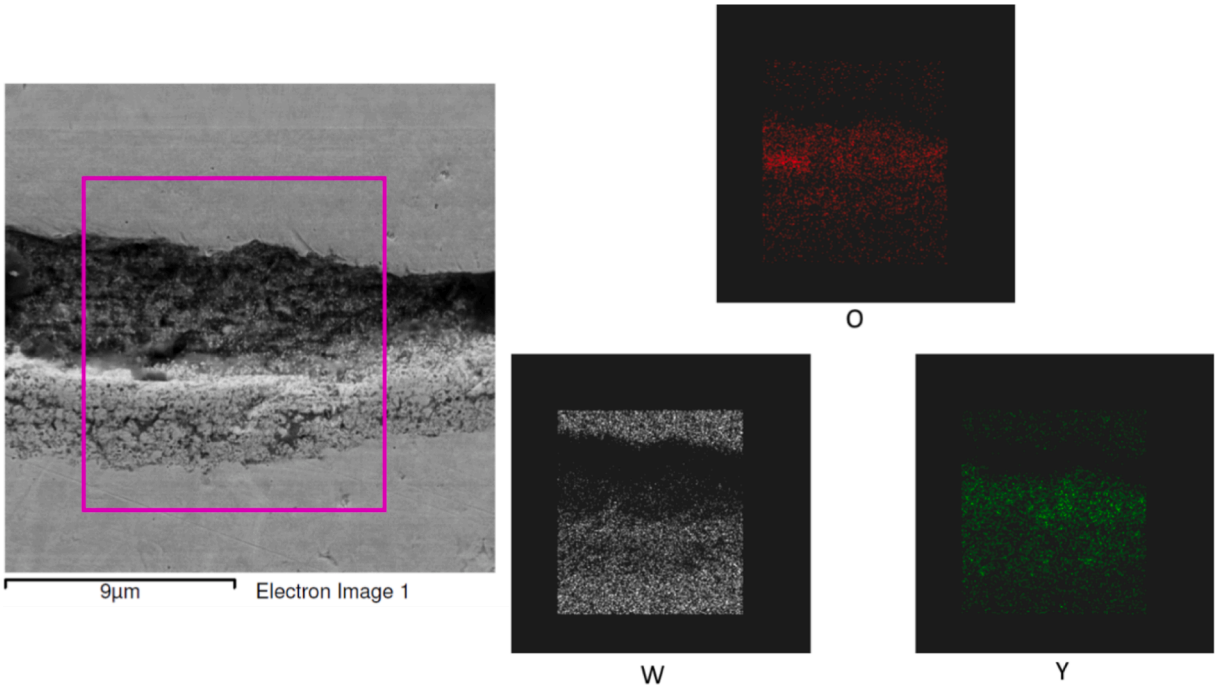

Fig. 10. EDS analysis on the interface region.

extra energy consumption mechanisms (can be seen in Fig. 12), e.g. interface debonding, fiber ductile deformation, fracture deflection, the sample give a high damage resilience. The key factor to realize these extrinsic toughening mechanisms is the dedicated fiber/matrix interface [26]. As can be seen from Figs. 12, 7 out of 9 fibers are effectively debonded from the tungsten matrix and failed with necking effect. This promising fracture behavior prove that the EPD coated yttrium oxide layer can be used as the interface material for W_f/W. For the two fibers showing cleavage fracture (Fig. 12c), the interface is visible and certain amount of interface debonding can be observed, but the fibers still broke without necking effect. However, it doesn't mean these two fibers failed totally in a brittle manner without any ductile deforemation. Two possible explanation for the missing of the necking effect: 1, the interface for these two fibers are too strong due to the damage of the interlayer during CVD, which limiting the necking behavior of the fibers; 2, there is a local difference in terms of strain rate, these two fibers faced too quick strain rate before they can fully perform their ductility.

Conclusion

This process is administered with various parameters like Zeta potential of the nanoparticles, dispersion stability, applied electric field, deposition time, deposition conditions, etc., which are needed to be altered to successfully implement EPD. In this work, the colloidal dispersion was obtained from the yttria nanoparticle slurry. As per the Zeta potential analysis, the deposition was Anodic. During the deposition (anodic) process at higher deposition voltage, it was seen that the tungsten was oxidized. The structural analysis of the coating by FIB-SEM demonstrates the porosity of the coating structure. The porosity of the achieved yttria coatings is because the nanoparticles are just simple stacked on another without any densification (melting/sintering etc.). The effect of annealing step on the EPD coated specimens indicated no change in the microstructure of the yttria coating. However, the high porosity could lead to a stress redistribution during the annealing process, avoiding the coating delamination. The deposition on the tungsten

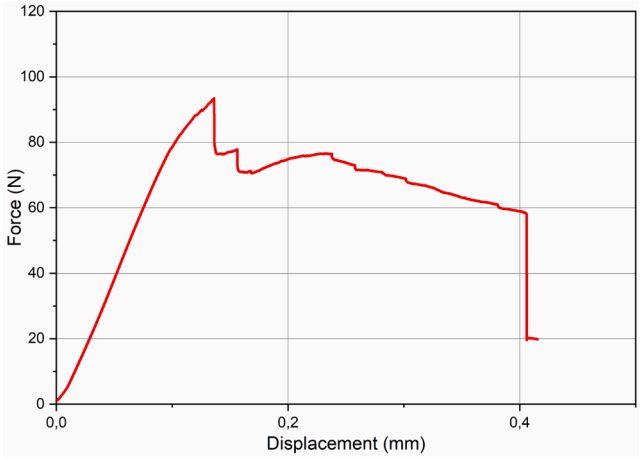

Fig. 11. Typical force displacement curves for 3-point bending test for the single layer W_f/W composites.

wire substrates at lower voltages ranging from 10 V to 30 V showed stable coating on the substrate surface. However, the FIB-SEM analysis of the specimens deposited at 30 V DC showed a sub-micron layer that was not present in the rest of the specimens. The EPD coated W weaves are used to prepare a single layer Wf/W composites by CVD process. The EPD coating can efficiently separate the W fibers and W matrix, which allows for a pseudo-ductile behavior.

CRediT authorship contribution statement

Y. Mao: Conceptualization, Investigation, Writing – original draft, Writing – review & editing. **A. Duggal:** Methodology, Investigation, Conceptualization. **A. Dittes:** Methodology, Investigation, Validation. **T. Lampke:** Resources, Project administration. **J.W. Coenen:** Supervision, Validation. **Ch. Linsmeier:** Resources, Funding acquisition, Project administration.

Declaration of Competing Interest

The authors declare that they have no known competing financial interests or personal relationships that could have appeared to influence the work reported in this paper.

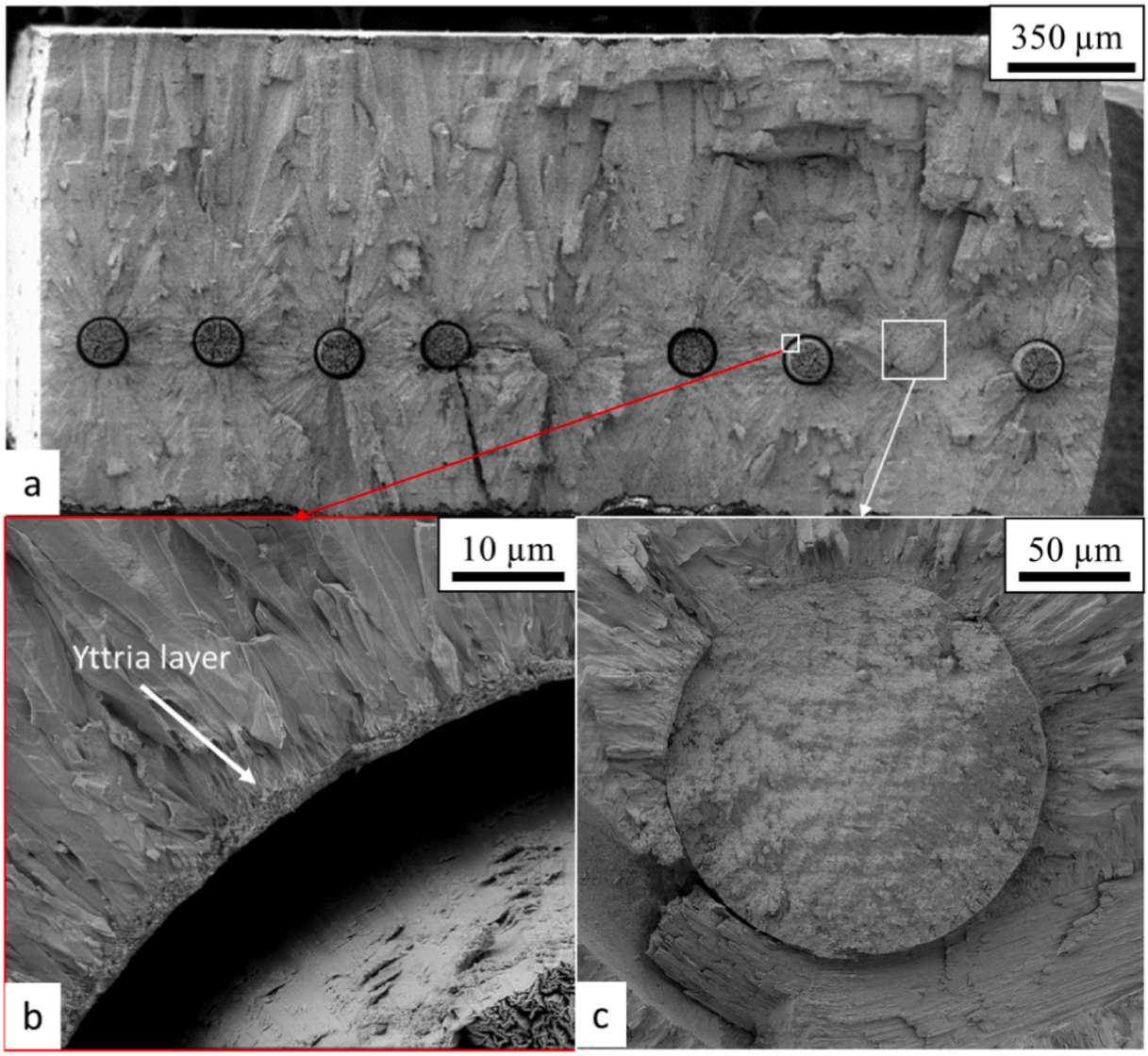

Fig. 12. The fracture section after 3-point bending test on the single layer w_f/W, a) the overview, b) the fiber/interface region with a ductile fiber fracture, c) the fiber/interface region with a brittle fiber fracture.

Data availability

Data will be made available on request.

Acknowledgments

This work has been carried out within the framework of the EUROfusion Consortium, funded by the European Union via the Euratom Research and Training Programme (Grant Agreement No 101052200 - EUROfusion). Views and opinions expressed are however those of the author(s) only and do not necessarily reflect those of the European Union or the European Commission. Neither the European Union nor the European Commission can be held responsible for them.

References

[1] H. Bolt, V. Barabash, W. Krauss, J. Linke, R. Neu, S. Suzuki, N. Yoshida, A.U. Team, Materials for the plasma-facing components of fusion reactors, J. Nucl. Mater. 329–333 (2004) 66–73.
[2] V. Philipps, Tungsten as material for plasma-facing components in fusion devices, J. Nucl. Mater. 415 (1) (2011) S2–S9.
[3] J.W. Coenen, S. Antusch, M. Aumann, W. Biel, J. Du, J. Engels, S. Heuer, A. Houben, T. Hoeschen, B. Jasper, F. Koch, J. Linke, A. Litnovsky, Y. Mao, R. Neu, G. Pintsuk, J. Riesch, M. Rasinski, J. Reiser, M. Rieth, A. Terra, B. Unterberg, W. Th, T. Wegener, J.H. You, L. Ch, Materials for DEMO and reactor applications—boundary conditions and new concepts, Phys. Scr. 2016 (T167) (2016), 014002.
[4] G. Pintsuk, I. Bobin-Vastra, S. Constans, P. Gavila, M. Rödig, B. Riccardi, Qualification and post-mortem characterization of tungsten mock-ups exposed to cyclic high heat flux loading, Fusion Eng. Des. 88 (9–10) (2013) 1858–1861.
[5] J. Riesch, J.Y. Buffiere, T. Höschen, M. di Michiel, M. Scheel, C. Linsmeier, J. H. You, In situ synchrotron tomography estimation of toughening effect by semi-ductile fibre reinforcement in a tungsten-fibre-reinforced tungsten composite system, Acta Mater. 61 (19) (2013) 7060–7071.
[6] Y. Mao, J.W. Coenen, J. Riesch, S. Sistla, J. Almanstötter, J. Reiser, A. Terra, C. Chen, Y. Wu, L. Raumann, T. Höschen, H. Gietl, R. Neu, C. Linsmeier, C. Broeckmann, Fracture behavior of random distributed short tungsten fiber-reinforced tungsten composites, Nucl. Fusion 59 (8) (2019), 086034.
[7] H. Gietl, J. Riesch, J.W. Coenen, T. Hoschen, C. Linsmeier, R. Neu, Tensile deformation behavior of tungsten fibre-reinforced tungsten composite specimens in as-fabricated state, Fusion Eng. Des. 124 (2017) 396–400.
[8] Y. Mao, J.W. Coenen, J. Riesch, S. Sistla, J. Almanstotter, B. Jasper, A. Terra, T. Hoschen, H. Gietl, C. Linsmeier, C. Broeckmann, Influence of the interface strength on the mechanical properties of discontinuous tungsten fiber-reinforced tungsten composites produced by field assisted sintering technology, Compos Part a-Appl S 107 (2018) 342–353.
[9] J. Riesch, Y. Han, J. Almanstotter, J.W. Coenen, T. Hoschen, B. Jasper, P. Zhao, C. Linsmeier, R. Neu, Development of tungsten fibre-reinforced tungsten composites towards their use in DEMO-potassium doped tungsten wire, Phys. Scr. T167 (T167) (2016), 014006.
[10] Y. Mao, J. Engels, A. Houben, M. Rasinski, J. Steffens, A. Terra, C. Linsmeier, J. W. Coenen, The influence of annealing on yttrium oxide thin film deposited by reactive magnetron sputtering: Process and microstructure, Nuclear Materials and Energy 10 (2017) 1–8.
[11] F. Yan, Z. Liu, W. Liu, Structural and optical properties of yttrium trioxide thin films prepared by RF magnetron sputtering, Vacuum 86 (1) (2011) 72–77.
[12] R. Forrest, A. Tabasso, C. Danani, S. Jakhar, A. Shaw, Handbook of activation data calculated using EASY-2007, UKAEA FUS 552 (2009) 399.
[13] P. Lei, J. Zhu, Y. Zhu, C. Jiang, X. Yin, Yttrium oxide thin films prepared under different oxygen-content atmospheres: microstructure and optical properties, Appl. Phys. A 108 (3) (2012) 621–628.
[14] J. Lyklema, Fundamentals of interface and colloid science: soft colloids, Elsevier, 2005.
[15] S. Heavens, Electrophoretic deposition as a processing route for ceramics, Noyes Publications, Advanced Ceramic Processing and Technology. 1 (1990) 255–283.
[16] L. Besra, M. Liu, A review on fundamentals and applications of electrophoretic deposition (EPD), Prog. Mater Sci. 52 (1) (2007) 1–61.
[17] H. Hamaker, Formation of a deposit by electrophoresis, Trans. Faraday Society 35 (1940) 279–287.
[18] L. Kremser, D. Blaas, E. Kenndler, Capillary electrophoresis of biological particles: viruses, bacteria, and eukaryotic cells, Electrophoresis 25 (14) (2004) 2282–2291.
[19] W. Schmickler, Electrochemical Theory: Double Layer, Reference Module in Chemistry, Molecular Sciences and Chemical Engineering, Elsevier, 2014.
[20] A.J. Shnoudeh, I. Hamad, R.W. Abdo, L. Qadumii, A.Y. Jaber, H.S. Surchi, S. Z. Alkelany, Chapter 15 - Synthesis, Characterization, and Applications of Metal Nanoparticles, in: R.K. Tekade (Ed.), Biomaterials and Bionanotechnology, Academic Press, 2019, pp. 527–612.
[21] D. Hanaor, M. Michelazzi, C. Leonelli, C.C. Sorrell, The effects of carboxylic acids on the aqueous dispersion and electrophoretic deposition of ZrO2, J. Eur. Ceram. Soc. 32 (1) (2012) 235–244.
[22] S. Prabhu, K. Murugan, Zeta potential measurements in colloidal suspensions, Int. Conf. Syst. Sci. Control. Commun. Eng. Technol (2015) 224.
[23] H. Gietl, S. Olbrich, J. Riesch, G. Holzner, T. Höschen, J.W. Coenen, R. Neu, Estimation of the fracture toughness of tungsten fibre-reinforced tungsten composites, Eng. Fract. Mech. 232 (2020), 107011.
[24] H. Miyazaki, A. Ichikawa, H. Suzuki, T. Ota, Influence of Deposition Condition on Y2O3Coatings Produced by Pulsed Electrophoretic Deposition, Adv. Mater. Sci. Eng. 2016 (2016) 1–7.
[25] H. Gietl, J. Riesch, M. Zielinski, T. Höschen, J.W. Coenen, S. Schönen, R. Neu, Interlayer properties of tungsten fibre-reinforced composites and their determination by different methods, Nuclear Materials and Energy 28 (2021).
[26] R. Shu, Y. Mao, J.W. Coenen, A. Terra, C. Liu, S. Schönen, J. Riesch, C. Linsmeier, C. Broeckmann, Interface and mechanical properties of the single-layer long fiber reinforced Wf/W composites fabricated via field assisted sintering technology, Mater. Sci. Eng. A 857 (2022), 144098.